SCIENCE CHINA
Earth Sciences

• RESEARCH PAPER •

September 2014 Vol.57 No.9: 2242–2258
doi: 10.1007/s11430-014-4910-8

Influence of advection on the characteristics of turbulence over uneven surface in the oasis and the Gobi Desert

CHEN JinBei*, HU YinQiao, LÜ ShiHua & YU Ye

Key Laboratory of Land Surface Process and Climate Change in Cold and Arid Regions; Cold and Arid Regions Environment and Engineering Institute, Chinese Academy of Sciences, Lanzhou 730000, China

Received December 17, 2013; accepted March 10, 2014; published online June 24, 2014

Utilizing experimental data of the atmospheric surface layer in the Gobi Oasis of Jinta in a comparative study, we demonstrate that under the condition of unstable stratification, the normalization variances of temperature in the oasis and Gobi Desert meet $\varphi_\theta(z/\Lambda)=\alpha_\theta(-z/\Lambda)^{-1/3}$ while normalization variances of both humidity and CO_2 in the oasis meet $\varphi_s(z/\Lambda)=\alpha_s(1-\beta_s z/\Lambda)^{-1/3}$; the normalization variance of temperature in the oasis is large due to disturbance by advection, whereas variance of CO_2 in the Gobi Desert has certain degree of deviation relative to Monin-Obukhov (M-O) scaling, and humidity variance completely deviates from variance M-O scaling. The above result indicates that under the condition of advection, humidity variance meets the relation $\sigma_{sm}^2=D^2\sigma_{sA}^2+\sigma_{sB}^2$ and it is determined by relative magnitude of scalar variance of advection transport. Our study reveals that, if the scalar variance of humidity or CO_2 transported by advection is much larger than local scalar variance, observation value of scalar variance will deviate from M-O scaling; when scalar variance of advection transport is close to or less than local scalar variance, the observation value of scalar variance approximately meets M-O scaling.

atmospheric surface layer (ASL), turbulence similarity theory, advection, uneven surface

Citation: Chen J B, Hu Y Q, Lü S H, et al. 2014. Influence of advection on the characteristics of turbulence over uneven surface in the oasis and the Gobi Desert. Science China: Earth Sciences, 57: 2242−2258, doi: 10.1007/s11430-014-4910-8

For the turbulent scalar transport in the atmospheric surface layer (ASL) under the condition of homogeneous surface and steadiness, classic Monin-Obukhov similarity theory (MOST) (Monin et al. 1954) has authentically disclosed the dynamic and thermal mechanisms of the scalar transport. Moreover, Monin-Obukhov (M-O) scaling also has effectively described the structure characteristics of turbulence (Stull, 1988). Based on MOST and M-O scaling, a flux-variance (FV) (Hill, 1989) scaling has been developed and used to estimate turbulent flux and explore similarities in sources and sinks at the ground surface (Katul et al., 1995; Finnigan, 2008; Townsend, 1961; Asanuma et al., 1999; De Bruin et al., 1999; Guo et al., 2009). Turbulent transport theory under ideal conditions is growing mature, but a theoretical framework that interprets scaling properties for heterogeneous surface is lacking (Finnigan, 2008; Detto et al., 2008). In the past half a century, amounts of experiments have revealed some properties of the M-O scaling under various complex conditions. Dynamic and thermal processes together determined the generation and development of turbulence (Hu et al., 2007). M-O scaling of temperature is more efficient than that of humidity and CO_2 due to the sensitivity of scalar to land surface changes (Katul et al., 1995). The variances of horizontal and longitudinal wind velocities more deviate from M-O scaling than the variance of vertical

*Corresponding author (email: chenjinbei@lzb.ac.cn)

wind velocity (Detto et al., 2010). The turbulence phase difference of scalars and their flux distribution difference strongly influence the turbulent characteristics of the scalars of humidity and CO_2. The phase differences among the scalar fluctuations and relevant flux distributions strongly affect the turbulent characteristics of the scalar, such as humidity, CO_2, etc. (Hill, 1989; Asanuma et al., 1999; De Bruin et al., 1999). The scalar turbulent fluctuations linked with eddy sizes that are comparable to the scales of source heterogeneity result in the deviation from M-O scaling (Detto et al., 2008). In the direction of the wind from scalar sources, the advection transport allows random plumes to occasionally arrive at the point of measurement, resulting in complex and highly non-stationary patterns in time traces of scalar concentration (Detto et al., 2010). In addition, in the very stable boundary layer, the scaling properties of vectors and scalars are commonly complicated by other non-turbulent mechanisms so that the applicability of MOST is doubted (Mahrt, 1989; Mahrt et al., 1998; McNaughton et al., 1998; Lamaud et al., 2006). Based on these findings, it is proposed that the global statistics of scalar fluctuations may be decomposed into a local component that tracks most likely MOST scaling and a non-local component introduced by exogenous factors, such as the heterogeneity and advection variability, which force the scalar away from the equilibrium state of turbulence (Detto et al., 2010).

Under the idealized conditions of atmosphere and land homogeneity, the M-O theory is comparatively more valid. However, the surface in nature is variable, and turbulent transfer under complex conditions has already become an urgent issue (Zhang et al., 2001). There are significant dynamic and thermal differences between the complex vegetation system of oasis and the flat gravel surface of Gobi Desert (Hu et al., 1988), and their material and energy are interchanged by means of advective and turbulent flows. Two sets of experimental data taken from over the heterogeneous surface in an oasis and the Gobi Desert, as well as the homogeneous surface of the Qinghai-Tibet Plateau, are applied to compare and analyze the M-O scaling of wind velocity variance and scalar variances of temperature, moisture and CO_2, thereby revealing the structure characteristics and physical mechanisms of turbulence under different conditions of surfaces. The influence of advection on the scalar variances is also analyzed by spectral analysis. Finally, based on several assumptions, a possible physical mechanism for the influence of advection on M-O scaling is discussed under the condition of heterogeneous surface of the oasis and Gobi Desert.

1 Theory

1.1 Local similarity scaling in surface layer

In the oasis and Gobi Desert, the main characteristics include the advection transportation of heat and material, thermal convection of the Gobi Desert and stable boundary layer of the oasis in the daytime, due to their typical complex surfaces. The MOST mainly is applied to the homogeneous surface (Sorbian, 1989), but the local MOST is applied to the atmospheric boundary layer of the heterogeneous surface that undergoes advection. Moreover, the local MOST is also typically applied to describe the stable boundary layer and convection boundary layer (Shao et al., 1990; Hu et al., 1993a). So this study utilizes the local MOST.

Under ideal conditions, the local M-O scaling of wind velocity and scalars, such as temperature, can be written as

$$\sigma_i / u_* = \varphi_i\left(z / \Lambda\right), \qquad \left(i = u, v, w\right), \tag{1}$$

$$\sigma_s / \left|s_*\right| = \varphi_s\left(z / \Lambda\right), \qquad \left(s = \theta, q, \rho_c\right), \tag{2}$$

where σ refers to turbulent variance; the subscript i refers to the vectors u, v and w of wind velocity; s represents scalar as potential temperature θ, humidity q and CO_2 concentration ρ_c, etc.; u_* is the friction velocity, which is defined as $u_* = \left(\overline{u'w'}^2 + \overline{v'w'}^2\right)^{1/4}$; and s_* represents the turbulent characteristic quantity of the relevant scalar, which is defined as $s_* = -\overline{w's'}/u_*$. CO_2 variance is simplified as σ_c in this paper. The local M-O length Λ is

$$\Lambda = \frac{-u_*^3 \overline{\theta_v}}{\kappa g \overline{w'\theta_v'}}. \tag{3}$$

Many studies have demonstrated that under ideal conditions, $\varphi_i\left(z / \Lambda\right)$ and $\varphi_s\left(z / \Lambda\right)$ have the following forms for unstable stratification (Panofsky et al., 1977; Padro, 1993; Katul, 1999):

$$\varphi_i\left(z / \Lambda\right) = c_1\left(1 - c_2\, z/\Lambda\right)^{1/3}, \tag{4}$$

$$\varphi_s\left(z / \Lambda\right) = \alpha_s\left(1 - \beta_s\, z/\Lambda\right)^{-1/3}, \tag{5}$$

where c_1, c_2, α_s and β_s are undetermined coefficients. The corresponding functional relationship under the condition of free convection is as follows (Wyngaard et al., 1971; Högström et al., 1974; Kader et al., 1990):

$$\varphi_i\left(z / \Lambda\right) = c\left(-z/\Lambda\right)^{1/3}, \tag{6}$$

$$\varphi_s\left(z / \Lambda\right) = \alpha_s\left(-z/\Lambda\right)^{-1/3}. \tag{7}$$

c in eq. (6) is an undetermined coefficient. When satisfying $z / \Lambda = -0.04$, free convection begins to develop; when satisfying $-z / \Lambda \geqslant 0.04$, the temperature variance function satisfies eq. (7) (Wyngaard et al., 1971; Katul et al., 1995).

1.2 Spectral analysis of turbulence

The power spectrum and cospectrum can subtly describe the turbulent characteristics of different frequencies. In isotropic turbulence, the power spectra of wind velocity and other scalars satisfy the Kolmogorov –5/3 scaling law (Stull, 1988):

$$S_i(\kappa) = C_i \varepsilon_i^{2/3} \kappa^{-5/3}, \tag{8}$$

$$S_s(\kappa) = C_s \varepsilon_s^{-1/3} \kappa^{-5/3}, \tag{9}$$

where $S(\kappa)$ represents the power spectrum corresponding to wave number κ; C is an undetermined coefficient; and ε is the turbulent dissipation rate.

In addition, Oncley et al. (1996) defines a frequency cumulative integral Ogive function of the cospectrum as

$$Og_{x,y}(f_0) = \int_{\infty}^{f_0} Co_{x,y}(f)\mathrm{d}f. \tag{10}$$

$Co_{x,y}(f)$ is the cospectrum of $\overline{xy}$ (Jiang et al., 2013), i.e.,

$$Co_{x,y}(f) = \frac{1}{N}\sum_{k=0}^{N-1} x(k)\cos\left(\frac{2\pi nk}{N}\right)\frac{1}{N}\sum_{k=0}^{N-1} y(k)\cos\left(\frac{2\pi nk}{N}\right) + \frac{1}{N}\sum_{k=0}^{N-1} x(k)\sin\left(\frac{2\pi nk}{N}\right)\frac{1}{N}\sum_{k=0}^{N-1} y(k)\sin\left(\frac{2\pi nk}{N}\right), \tag{11}$$

where N represents the data volume and n is the cycle index. When sampling the interval equal to Δt, the frequency is $f = n/(N\Delta t)$. Eq. (10) is an integral equation from high- to low-frequency, (∞, f_0). As a function of frequency f_0, when frequency f_0 is sufficiently low, the Ogive function will tend to be a constant representing the function Ogive's tendency to be converged. Oncley et al. (1996) treat the Ogive function as the point of convergence to judge the ergodicity of the turbulence, and treat the corresponding time of frequency f_0 at the point of convergence as the average time scale of the turbulence. If Ogive converges at the point of frequency f_0, then eq. (10) can be used to describe the general trend of the cospectrum from high- to low-frequency f_0, (∞, f_0). The larger the absolute value of the Ogive curve slope is, the greater contribution the corresponding frequency to the cospectrum is. When the Ogive curve tends to be gradual, this signifies that a smaller contribution of the frequency band to the cospectrum has been made. Therefore, the proportion of high- and low-frequency components in the turbulent flux can be judged according to the Ogive frequency accumulative integrals. This paper analyzes the contribution of different frequency spectrum components to turbulent flux based on frequency accumulative integrals Ogive, and the results reveal the influence of low-frequency advection on the turbulence.

Finally, in order to more effectively analyze the effects of different frequency components (advection, large eddy or average vertical velocity) in the turbulence on the turbulent flux, the cospectrum and power spectrum were applied to determine the spectrum of the correlation coefficient in the piecewise intervals $[f_1, f_2]$, $[f_2, f_3]\ldots[f_{n-1}, f_n]$:

$$R_{w,s}(f) = \int_{f_1}^{f_2}\left[Co_{w,s}(f)\Big/\sqrt{S_w(f)S_s(f)}\right]\mathrm{d}f;\quad f_1 > f_2. \tag{12}$$

Previous researches have demonstrated that correlation coefficient increases as the frequency decreases from high- to low-frequency, reaches its maximum around the frequency of fz/U=0.1–0.01, and then subsequently begins to shock (McBean et al., 1972; Ricardo et al., 2001).

1.3 Influence of advection on scalar turbulence

The following predictive equation of scalar variance shows that the scalar variance may be transported by the advection and diffused and dissipated by the turbulence as well (Stull, 1988):

$$\frac{\partial\overline{s'^2}}{\partial t} + \overline{U_j}\frac{\partial\overline{s'^2}}{\partial x_j} = -2\overline{s'u'_j}\frac{\partial\overline{s}}{\partial x_j} - \frac{\partial\overline{\left(u'_j s'^2\right)}}{\partial x_j} - 2\varepsilon_s. \tag{13}$$

Over grids of different surfaces, Asanuma and Brutsaert (1999) proposed that the mixture of turbulent scalar variances originating from two different surfaces A and B becomes $\sigma_{sm}^2 = \frac{1}{2}\left(\sigma_{sA}^2 + \sigma_{sB}^2\right)$. Moene et al. (2006) suggested that, when the characteristic quantity of turbulent scalars is mixed through the entrainment process, there is a linear relation $s_{*c}^2 = as_*^2 + bs_{*e}^2$ among the mixed scalar variance s_{*c}, as well as scalar variance s_* at the mixing layer top and entrained scalar variance s_{*e}. All these mixture cases demonstrate that the turbulent scalar transported by different low frequency transport processes in the new turbulent flow field retains some information from the original turbulent flow field.

We first assume that the turbulent pulsation scalar formed in the flow field of upwind direction of zone A is s'_A, which meets eq. (5) or eq. (7). When the air mass reaches zone B after advection transport, s'_A decreases into Ds'_A, due to turbulent diffusion and dissipation, in which D is the decay rate. Meanwhile, a new turbulent pulsation s'_B has also been spurred in zone B. A simple linear accumulative relation is valid, and the scalar pulsation becomes $s'_{sm} = Ds'_A + s'_B$. Then the scalar variance is determined as

$$\sigma_{sm}^2 = \frac{1}{N}\sum_{i=1}^{N}\left(Ds'_A + s'_B\right)_i^2 = D^2\sigma_{sA}^2 + \sigma_{sB}^2 + 2DCov\left(s'_A s'_B\right), \tag{14}$$

where σ_{sm} is the turbulent variance of the scalar s after

being mixed; σ_{sA} and σ_{sB} are the variances of s'_A and s'_B, respectively; and $Cov(s'_A s'_B)$ refers to the covariance of s'_A and s'_B. If s'_A and s'_B are spurred by two completely different turbulent flow fields of zones A and B, there is no correlation between s'_A and s'_B, namely $Cov(s'_A s'_B) \approx 0$. Here eq. (14) can be simplified as

$$\sigma_{sm}^2 = D^2\sigma_{sA}^2 + \sigma_{sB}^2 . \quad (15)$$

Given that both s'_A and s'_B are spurred by local turbulence, they respectively meet the following local relations:

$$\sigma_{sA}/s_{*A} = \varphi_{sA}(z/\Lambda), \quad (16)$$

$$\sigma_{sB}/s_{*B} = \varphi_{sB}(z/\Lambda). \quad (17)$$

Furthermore, relations (15)–(17) and the experimental data can be used to determine the turbulent scalar variance and its decay rate *D* transported by advection.

$$D\sigma_{sA} = \sqrt{\sigma_{sm}^2 - \left[s_{*B}\varphi_{sB}(z/\Lambda)\right]^2}\ , \quad (18)$$

$$D = \sqrt{\sigma_{sm}^2 - \left[s_{*B}\varphi_{sB}(z/\Lambda)\right]^2}\Big/\sigma_{sA} . \quad (19)$$

Under the condition of steadiness, the following relation can be obtained by integrating relation (13) from x_1 and x_2:

$$\overline{s_2'^2} - \overline{s_1'^2} = \int_{x_1}^{x_2} \frac{1}{\overline{U_j}}\left[-2\overline{s'u'_j}\frac{\partial\bar{s}}{\partial x_j} - \frac{\partial\left(\overline{u'_j s'^2}\right)}{\partial x_j} - 2\varepsilon_s\right]\mathrm{d}x_j . \quad (20)$$

According to relation (20), for horizontal advection transport, turbulent scalar pulsation s'_A will satisfy the following relation:

$$D^2\overline{s_A'^2} - \overline{s_A'^2} = \left(D^2 - 1\right)\overline{s_A'^2}$$
$$= \int_{x_A}^{x_B} \frac{1}{\overline{V}}\left[-2\overline{s'u'}\frac{\partial\bar{s}}{\partial x} - \frac{\partial\left(\overline{u's'^2}\right)}{\partial x} - 2\varepsilon_s\right]\mathrm{d}x, \quad (21)$$

where $\overline{V}$ is a one-dimensional horizontal wind velocity. It can be learned that $\left(D^2 - 1\right) \sim 1/\overline{V}$ in terms of relation (21) and $0<D<1$, then *D* will increase with the increase of $\overline{V}$. In addition, it is estimated that, with stronger turbulent dissipation, the turbulent scalar variance decreases, and decay rate *D* also decreases.

2 Experiments and data processing

2.1 Experimental locations

The Jinta Oasis, located in Gansu Province, China, is an artificial oasis irrigated by mountain snowmelt water from the Qilian Mountains. It is situated between 39.1°–40.28°N and 98.65°–99.13°E, with an area of 1652.2 km^2. The terrain in the oasis-Gobi area is flat and the altitude difference is only about 80 m. The oasis is less influenced by terrain, as it is located relatively far away from the Qilian Mountains. In the southernmost area of the oasis is lush vegetation irrigated by the reservoir of Yuanyang Lake. The lake water is transported by several canals flowing northeastward and northwestward. Patchy *Populus euphratica* and *Salix microstachya* forests grow around the canals. The entire oasis presents a regular triangle shape, and the observation area is located in the southernmost corner of the oasis (Figure 1). In the experiment, a 20-m-high observation tower is located in the oasis (40.01°N, 98.93°E). There is a step farmland with three layers and fall of about 1–2 m located below the tower, in which multiple crops such as cotton, wheat, tomato, and maize are alternately planted. On the southeast and northwest sides of the farmland, at a distance of 400 m, windbreak is composed of two rows of trees with heights of 10 m. At a distance of about 550 m between the northeast and southwest, there are houses of 3 m in height. Another observation tower is set in the Gobi Desert (39.99°N, 98.97°E), which is located close to the oasis. The two observation towers are 3.66 km apart from each other, and the Gobi tower is about 590 m away from the nearest farmland.

In order to compare the turbulent characteristics of the homogeneous surface and more effectively analyze the influence of advection on the turbulence between the oasis and Gobi Desert, this paper selects the observation data of the surface layer in Naqu of the Qinghai-Tibet Plateau (Figure 1). In this area, the experimental area is flat and grass grows uniformly with a height of about 10 cm. The observation point is about 5 km from the nearest mountainous region.

2.2 Experimental apparatus

A set of eddy correlation systems was installed at the level of 10 m in the oasis tower. This system consists mainly of three-dimensional ultrasonic anemometers (CSAT3, Campbell, USA), and an open circuit CO_2/H_20 analysis meter (Li7500, Li-Cor, USA). The other two sets of the same observed systems were installed in the Gobi tower at the respective levels of 10 and 1.84 m. Meanwhile, the wind velocity, temperature and humidity sensors produced by Campbell Co. were used to perform gradient observations of the wind, temperature, and humidity. In the oasis tower, the gradient observation was composed of four floors, respectively at 2.0, 6.0, 13.2, and 19.10 m, and that in the Gobi tower was composed of six floors, i.e., 1.57, 2.8, 4.5, 8.0, 12.0 and 18.0 m. The observations were performed from June 11, 2008 to June 26, during which all the heights of the crops were lower than 0.6 m. All raw data of wind

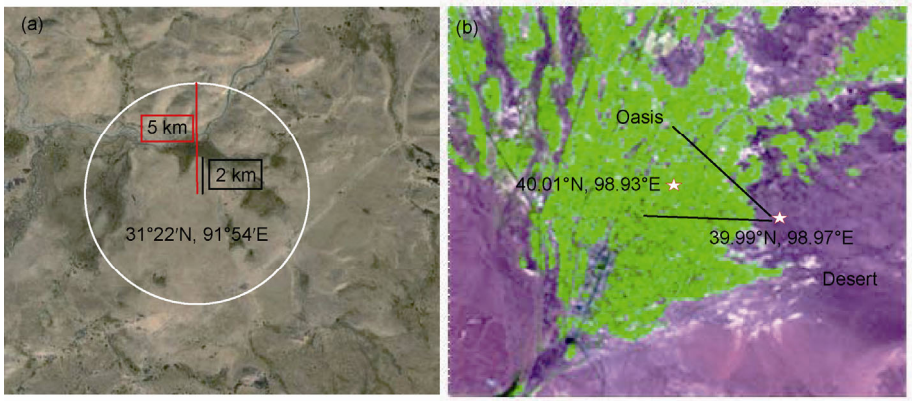

Figure 1 Sketch map of observation points.

velocity, temperature, humidity and CO_2 of 10 Hz were collected using the CR3000 and two sets of CR5000 produced by Campbell Co., and averaged for 30 min. Apart from cloudy skies on June 19 and 20, and dust on June 21, sunny weather persisted throughout the experimental period. In Naqu, at the Alpine Climate Environmental Observation Research Station of CAS, a set of the same eddy correlation system was applied. The turbulent characteristics observed at the level of 3.08 m from July 23 to September 13, 2011 over the uniform surface can be regarded as the comparison objects.

2.3 Data processing

Incorrect data were first deleted due to other reasons such as circuit pulse and dust. To eliminate the interference of the entrainment between the upper and lower layers in the advection effect research, when the turbulent flow filed the layers before and after the sunrise and sunset, the data excluded the data of 06:00–09:00 and 19:00–21:00 (Beijing time). In addition, the Gobi Desert has some stronger unstable stratification at night, which may be caused by cold advection and intermittent turbulence, and such data have also been excluded. Subsequently, the remaining data are corrected with the plane-fitting method. Separation between CSAT3 and Li7500 with time intervals of about 0.1 s is corrected through maximum correlation for 5 min, whereas ultrasonic temperature is corrected into absolute temperature (Schotanus et al., 1983; Kaimal et al., 1991). The humidity and CO_2 pulsation caused by air density fluctuation were not modified or corrected, because moisture and CO_2 are the components of air, their pulsations are also compositions of air density fluctuation, and the turbulent pulsation of air temperature is actualized by air molecule pulsation. It is clear to question the correction of the M-O scaling of humidity and CO_2 derived from the temperature pulsation, and the preliminary analysis reveals that such correction will cause the prediction to deviate from relations (4)–(7). Webb (1980) proposed that the average vertical velocity occurs when moisture runs over the surface after evaporation, while such vertical velocity may transport heat and mass, especially for moisture and CO_2. Therefore, Webb correction is ultimately used to estimate the vertical velocity and correct the covariance relevant to the turbulent flux. However, Webb correction involves the composition of surface energy balance, but it does not belong to the composition of turbulent flux ($-u_*s_*$). Therefore, in this study we did not perform Webb correction. Finally, the remaining data are 506 runs from 607 runs of the data from the oasis, in which there are 65 runs of unstable stratification. We also estimated displacement height d of 0.57 m by using the remaining data of the oasis (Martano, 2002). The respective data at 10 and 1.84 m in the Gobi tower are 607 and 515 runs, and the selected data are 479 and 405 runs, among which there are 303 and 312 runs of unstable stratification for each. Given the possible influences of the altitude height of the observation site and net radiation in Naqu on the results, the same correction process was repeated after the data collected during 05:00–09:00 and 18:00–21:00 (Beijing time) were excluded.

3 Results

3.1 Temperature and humidity distribution characteristics of the oasis and Gobi Desert

Boundary layers in the oasis are characterized by local circulation caused by the thermal difference between the oasis and its surrounding Gobi Desert, the temperature inversion in the internal boundary layer of the oasis, and the humidity inversion in the internal boundary layer of the Gobi Desert (Su et al., 1987; Hu et al., 1988; Hu et al., 1993b; Chen et al., 2012). Early research on the boundary layer of Jinta revealed that the heights of the internal boundary layer at daytime in summer can reach up to 500–800 m (Wei et al., 2005). Meanwhile, cold-wet tongues existing in the Gobi Desert close to the oasis also verified the height of the in-

ternal boundary layer of the Gobi Desert (Ao et al., 2005), ranging from 0 to 600 m. To understand the observational conditions and stratification characteristics of the surface layer in the oasis and Gobi Desert, the vertical profiles of the scalars and vertical wind velocity are first analyzed.

Figure 2 is the daily average vertical profile of temperature and humidity for each time in the oasis and Gobi Desert. The results show that there were mostly stable stratifications, aside from unstable stratification around 04:00–06:00 (Beijing time) in the oasis, which was caused by the influence of hot advection originating from the Gobi Desert in the daytime (Su et al., 1987; Hu et al., 1988; Hu et al., 1993b; Chen et al., 2012). Meanwhile, the eddy correction system in the oasis showed negative sensible heat fluxes (Su et al., 1987; Hu et al., 1988; Zhang et al., 1992). The average temperature profile of the Gobi Desert shows that the atmosphere in the daytime undergoes unstable stratification, and at that night undergoes stable stratification, but the average humidity profile in the Gobi Desert is relatively complex under the influence of moisture advection from the oasis. There is always a humidity high value area around 3 m, and the negative humidity gradient distribution can be found above 3 m. Meanwhile, the positive humidity gradient distribution and negative latent heat flux can often be found below 3 m. The influences of advection on the local atmospheric stratification were obvious, and it may be inferred that the observation heights in the two locations were respectively located in the internal boundary layers of the oasis and Gobi Desert. Moreover, after analyzing and comparing the average vertical velocity of 30 min, it is concluded that there is downward vertical velocity in the oasis in the daytime and upward average velocity in the Gobi Desert (Chen et al., 2012), thus verifying the local circulation occurring in these areas (figure omitted). This is consistent with the early observations and simulation results (Wen et al., 2005).

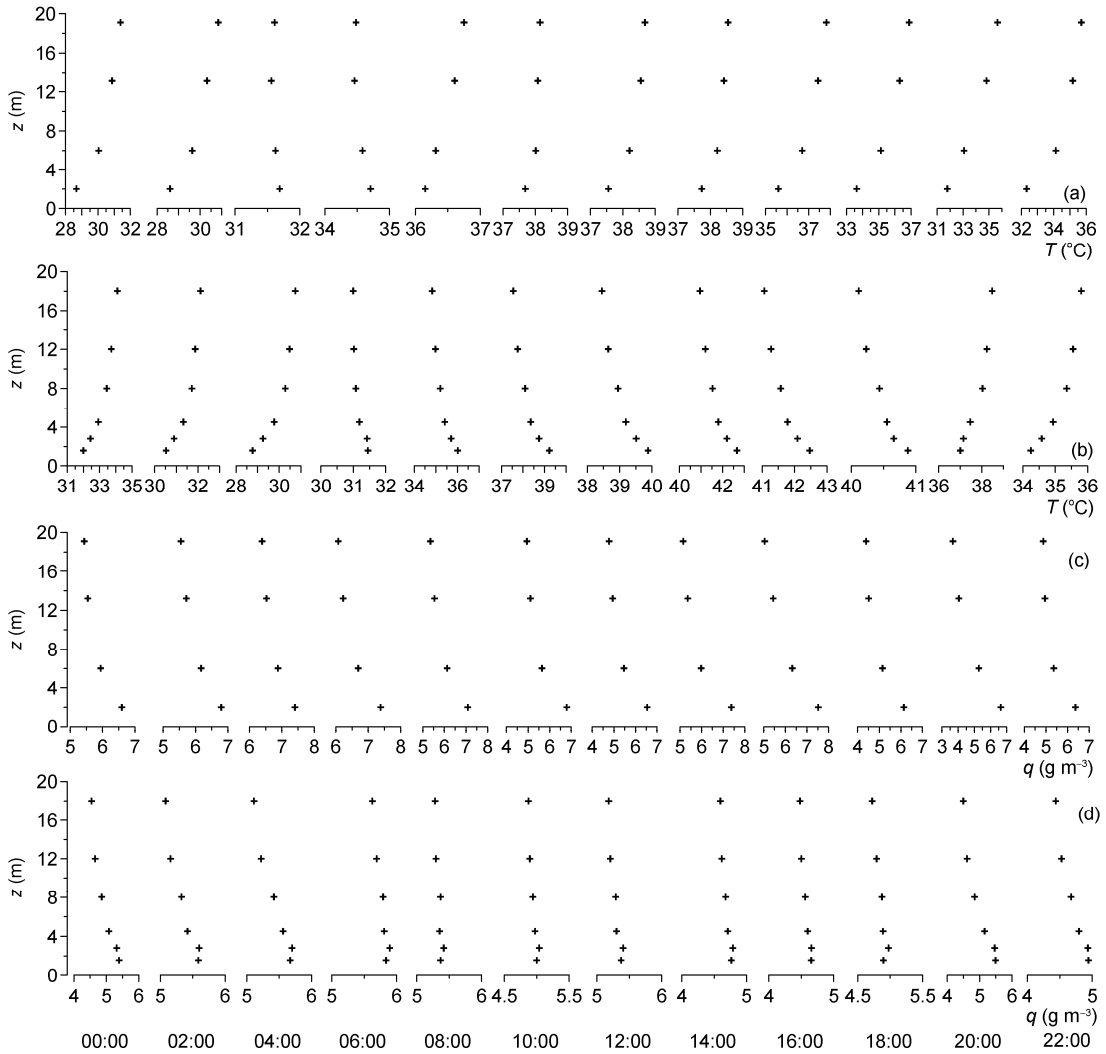

Figure 2 Average profile figure for each time of the temperature ((a), (b)) and humidity ((c), (d)) of the oasis and Gobi Desert.

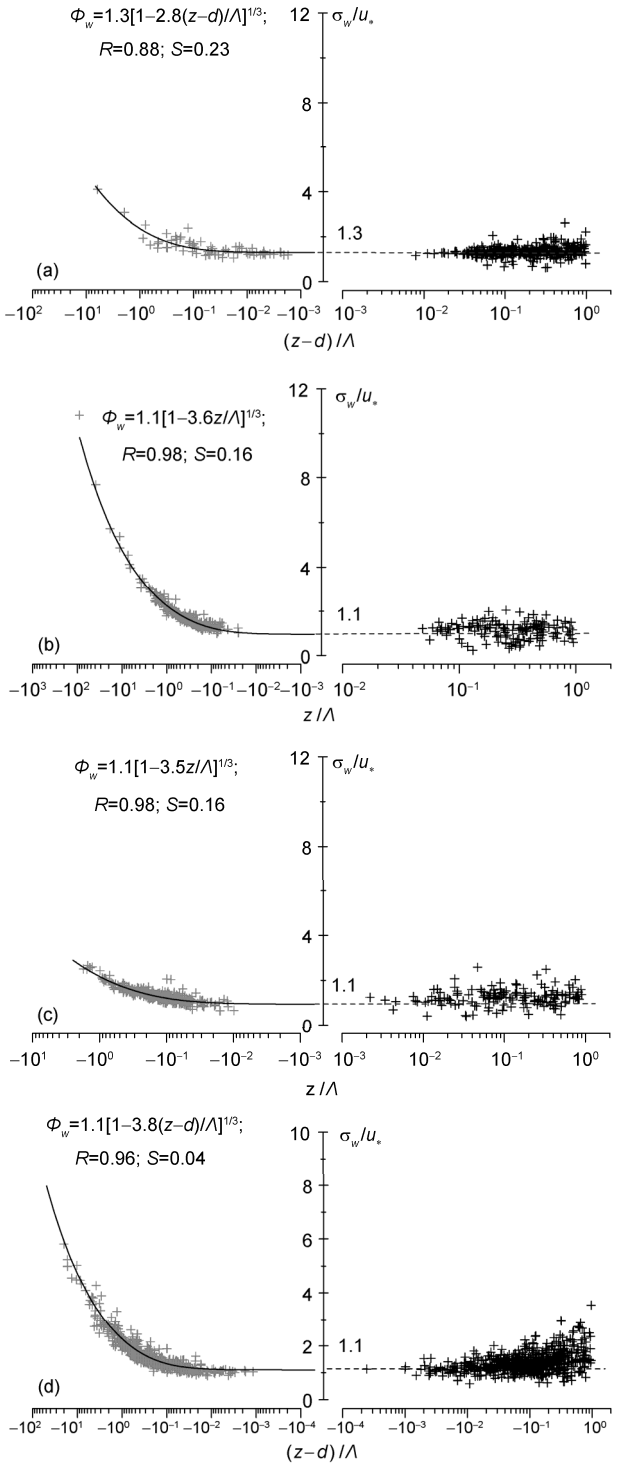

Figure 3 M-O scaling of vertical velocity w at level of 10 m (a) in the oasis, at 10 m (b) and 1.84 m (c) in the Gobi Desert, and at 3.08 m (d) in Naqu.

3.2 Turbulent M-O scaling in the oasis and Gobi Desert

3.2.1 M-O scaling of velocity

The velocity variance represents the turbulent kinetic energy and quantifies the turbulent intensity, thus we first analyze the M-O scaling of the velocity, the results of which are shown in Figure 3.

The primary cause of the turbulent development in the atmospheric boundary layer is the fact that the unequal heating of the sunlight on the ground leads to convection bubbles and causes turbulence. Then the vertical velocity variance becomes a basic characteristic quantity representing the turbulent development intensity. Figure 3 shows the M-O scaling of the vertical velocities at the levels of 10 m in the oasis, 10 and 1.84 m in the Gobi Desert, and 3.08 m over the homogeneous surface in Naqu. The M-O scalings of the velocities fitted by non-linear regression are shown in Table 1. Although the surfaces of the oasis and Gobi Desert are significantly different, and their atmospheric stratification influenced by the hot advection of the Gobi Desert is also relatively complex, the M-O scalings of the two observation points are fairly consistent with that in Naqu. Each figure shows that no matter whether unstable or stable stratification is present, the observation value of the vertical velocity variance is less deviated from the M-O scaling curve. The results indicate that the variation of the surface only has an influence on the magnitude of the vertical velocity normalized variances, and does not change the function form of the M-O scaling. This signifies that the surface condition cannot change the basic physical characteristics of the turbulence.

Figures 4 and 5 show the respective M-O scalings of longitudinal velocity u and horizontal velocity v at the same heights with vertical velocity w in the oasis, Gobi, and Naqu. The M-O scaling functions of longitudinal velocity u and horizontal velocity v, as well as their relevant correlation coefficients R and dispersion variances S, are listed in Table 1. Figures 4, 5 and Table 1 indicate that for unstable stratification, in both the oasis and Gobi Desert, both the variances of longitudinal velocity u and horizontal velocity v basically meet the M-O scaling. However, their function relations with smaller correlation coefficients and larger dispersion variance are worse than that of vertical velocity. In general, the correlation coefficients of the longitudinal and horizontal velocity M-O scaling, which respectively are R=0.54 and R=0.64, are lower in the oasis than in the Gobi Desert. Moreover, the correlation coefficients of the velocity M-O scaling, which respectively are R=0.84 and R=0.83, at the level of 10 m are larger than that at 1.84 m, with R=0.61 and R=0.64 in the Gobi Desert. The correlation coefficients of the velocity M-O scaling at the level of 1.84 m in the Gobi Desert are consistent with those at the level of 3.08 m in Naqu, which respectively are R=0.60 and R=0.64. These phenomena show that the effects of the surface dynamic heterogeneity on velocity M-O scaling are different. Because the surface of the oasis is more non-uniform than that of the Gobi Desert, the correlation coefficients of the M-O scaling fitting curve in the oasis are lower than those in the Gobi Desert. In addition, the observed area is farther

Table 1 M-O scaling of velocity components under the condition of unstable stratification

	Location/height (m)	M-O scaling	Correlation coefficient	Dispersion variance
Vertical velocity w	Oasis /10	$\Phi_w=1.3[1-2.8(z-d)/\Lambda]^{1/3}$	R=0.88	S=0.23
	Gobi /10	$\Phi_w=1.1(1-3.6z/\Lambda)^{1/3}$	R=0.98	S=0.16
	Gobi /1.84	$\Phi_w=1.1(1-3.5z/\Lambda)^{1/3}$	R=0.86	S=0.16
	Naqu /3.08	$\Phi_w=1.1[1-3.8(z-d)/\Lambda]^{1/3}$	R=0.86	S=0.16
Longitudinal velocity u	Oasis /10	$\Phi_u=2.6[1-0.8(z-d)/\Lambda]^{1/3}$	R=0.54	S=0.67
	Gobi /10	$\Phi_u=2.1(1-5.7z/\Lambda)^{1/3}$	R=0.84	S=1.23
	Gobi /1.84	$\Phi_u=3.5(1-3.8z/\Lambda)^{1/3}$	R=0.61	S=0.99
	Naqu /3.08	$\Phi_u=2.8[1-7.2(z-d)/\Lambda]^{1/3}$	R=0.60	S=2.37
Horizontal velocity v	Oasis /10	$\Phi_v=2.5[1-1.7(z-d)/\Lambda]^{1/3}$	R=0.64	S=0.75
	Gobi /10	$\Phi_v=2.1(1-7.1z/\Lambda)^{1/3}$	R=0.83	S=1.38
	Gobi /1.84	$\Phi_v=2.9(1-12.1z/\Lambda)^{1/3}$	R=0.64	S=1.41
	Naqu /3.08	$\Phi_v=2.8[1-6.2(z-d)/\Lambda]^{1/3}$	R=0.64	S=2.12

away from the ground, and thus the influence of terrain on the turbulence flow is less significant in the Gobi Desert.

3.2.2 *M-O scaling for temperature*

Because of the differences among the temperature and humidity characteristics of the upwind airflows at the two observational sites, the normalized variances have been classified and compared in terms of different wind directions before analyzing the M-O scaling of the temperature, humidity, and CO_2. The results show that the airflows, whether blowing from the sector receiving wind at 45°–315° or forest patches of *Populus euphratica* and red grahame in the northern area of the oasis, are both hot and dry. As far as the observation site in the Gobi Desert is concerned, it is easily affected by the local oasis-Gobi Desert circulation because of the proximity of its location to the oasis and being surrounded from three sides by the oasis. The M-O scaling of the temperature, humidity, and CO_2 does not vary consistently with the different wind directions. Therefore, in the following analysis of scalar variance the data are not classified in terms of different wind directions.

We also observed that the characteristic quantity s_* of the vertical turbulent flux varies positively and negatively with the direction of the flux, and the scatter plot of the normalized variance should be in the first and third quadrants of the coordinate system. This is because the variance is positive and the normalization processing by using π similar theory should not change the turbulent properties. Moreover, in order to compare and analyze the properties of the scalar variances close to the condition of neutral stratification, $-\sigma_\theta/\theta$ and σ_θ/θ_* are respectively selected when the temperature variance is in the unstable and stable stratifications, with $\sigma_q/|q_*|$ and $\sigma_c/|\rho_{c*}|$ being used for relatively complex humidity and CO_2 variance.

Figure 6 shows the M-O scaling for temperature in the oasis and Gobi Desert. Under the condition of unstable stratification, the respective M-O scaling fitting curves of temperature at the level of 10 m in the oasis, and 10.0 and 1.84 m in the Gobi Desert are $-\sigma_\theta/\theta_*=3.6[-(z-d)/\Lambda]^{-1/3}$, $-\sigma_\theta/\theta_*=1.1(-z/\Lambda)^{-1/3}$ and $-\sigma_\theta/\theta_*=1.0(-z/\Lambda)^{-1/3}$. The M-O scaling of temperature in the Gobi Desert is characterized by a high correlation coefficient, R=0.86 at the level of 10 m and R=0.90 at 1.84 m, and small dispersion (respectively S=0.26 and S=0.23), which is more coincident with the M-O scaling fitting curve of $-\sigma_\theta/\theta_*=1.2[-(z-d)/\Lambda]^{-1/3}$ (R=0.86 and S=0.64) in Naqu. The oasis is characterized by relatively larger magnitudes of $-\sigma_\theta/\theta$, lower correlation coefficient of M-O scaling fitting curve, and larger dispersion due to the influence of the thermal advection from the Gobi Desert. The dispersion variance even reaches as high as S=6.00, in spite of the correlation coefficient of R=0.70, as the magnitude of φ_θ is integrally ten times the size of that of the Gobi Desert. With regard to the condition of stable stratification, all the M-O scaling fitting curves of the temperature in the oasis and Gobi Desert exhibit a large dispersion. In the oasis, the cross points between the M-O scaling fitting curves and axis of ordinates from the stable to unstable stratifications are different and discontinuous, and all σ_θ/θ are less than the constant values predicted by the M-O scaling under the condition of stable stratification. Inferred in light of the vertical profile of the Gobi Desert humidity shown in Figure 2, the low-level air in the Gobi Desert is affected by the cold wet advection from the oasis, which strengthens the instability of the Gobi Desert stratification, in turn possibly causing the turbulence to undergo more sufficient development, and characterizes the M-O scaling of temperature at 1.84 and 10.0 m in the Gobi Desert with a small dispersion under the condition of unstable stratification.

3.2.3 *M-O scaling properties for CO_2*

During the experimental period, the decreased amount of CO_2 in the oasis, along with the sink of CO_2 (Hu et al., 1993), was less than 25% than the CO_2 density of the Gobi Desert. Figure 7 shows the M-O scaling of CO_2 in the oasis and Gobi Desert. As shown in the results, under the condition of unstable stratification, the CO_2 variance at 10 m in the oasis meets the M-O scaling of $\sigma_c/|\rho_{c*}|=$

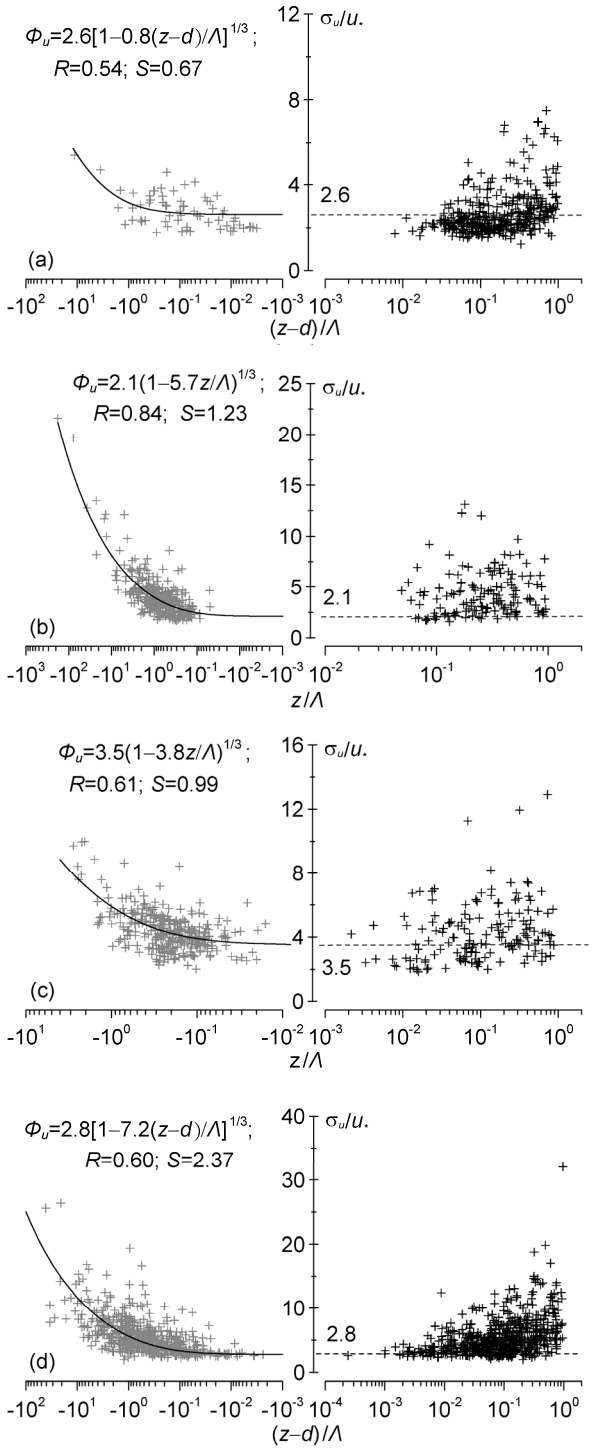

Figure 4 M-O scaling of the longitudinal velocity u at level of 10 m (a) in Oasis, at levels of 10 m (b) and 1.84 m (c) in Gobi (d), and at levels of 3.08 m in Naqu.

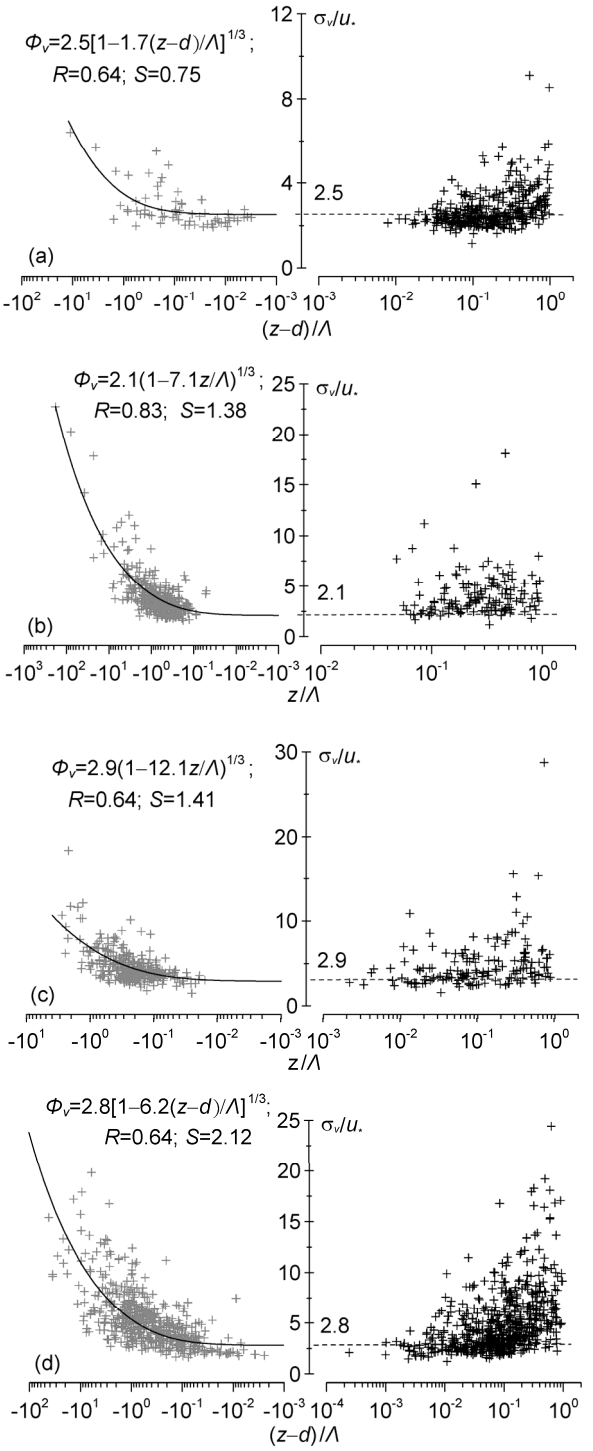

Figure 5 M-O scaling of horizontal velocity v at level of 10 m (a) in the oasis, at 10 m (b) and 1.84 m (c) in the Gobi Desert, and 3.08 m (d) in Naqu.

$2.1\left[1-9.8\left(z-d\right)/\Lambda\right]^{-1/3}$, while those at 1.84 and 10.0 m in the Gobi Desert meet the relations of $\sigma_c/\left|\rho_{c^*}\right|=3.3\left(1-18.6\,z/\Lambda\right)^{-1/3}$ and $\sigma_c/\left|\rho_{c^*}\right|=2.6\left(1-8.1\,z/\Lambda\right)^{-1/3}$. The CO_2 variance at 10 m in the oasis preferably complies with the MOST, which is characterized by having a higher correlation coefficient and smaller dispersion. However, the CO_2 variance at 1.84 m in the Gobi Desert deviates slightly from the M-O scaling, and the CO_2 variances at 10 m the Gobi Desert are consistent with the prediction of the M-O scaling, except for 24 points deviating from the M-O scaling.

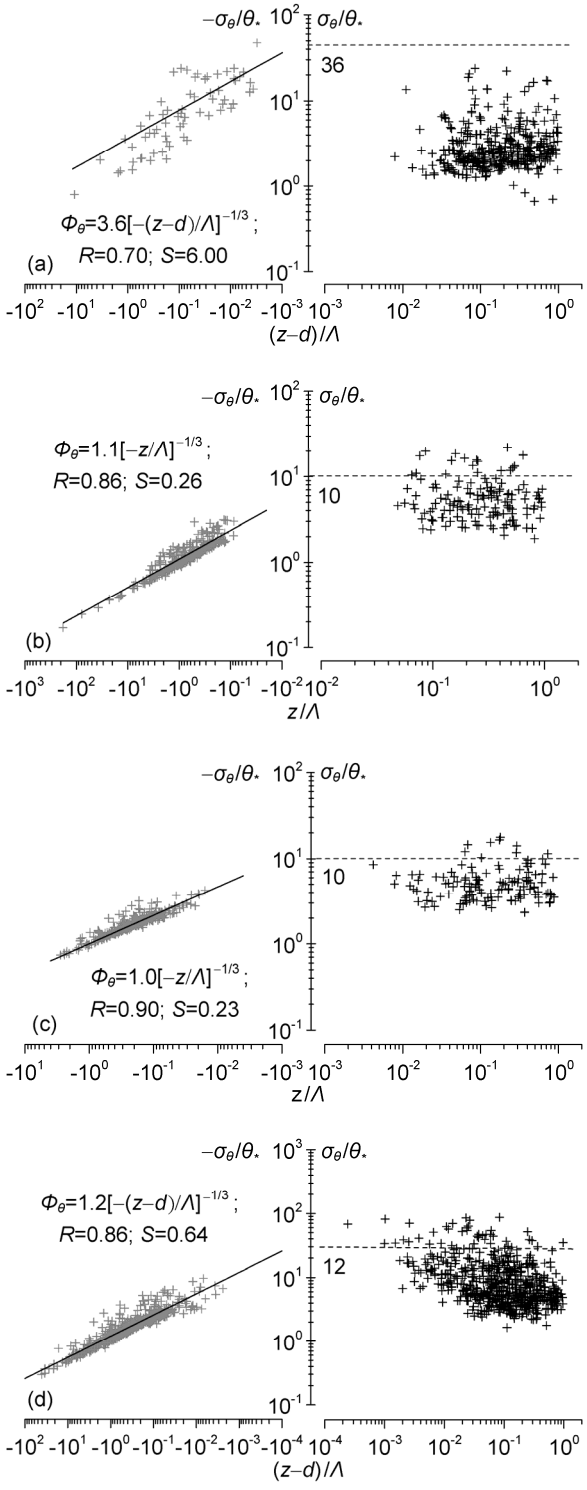

Figure 6 M-O scaling for temperature at level of 10 m (a) in the oasis, 10 m (b) and 1.84 m (c) in the Gobi Desert, and 3.08 m (d) in Naqu.

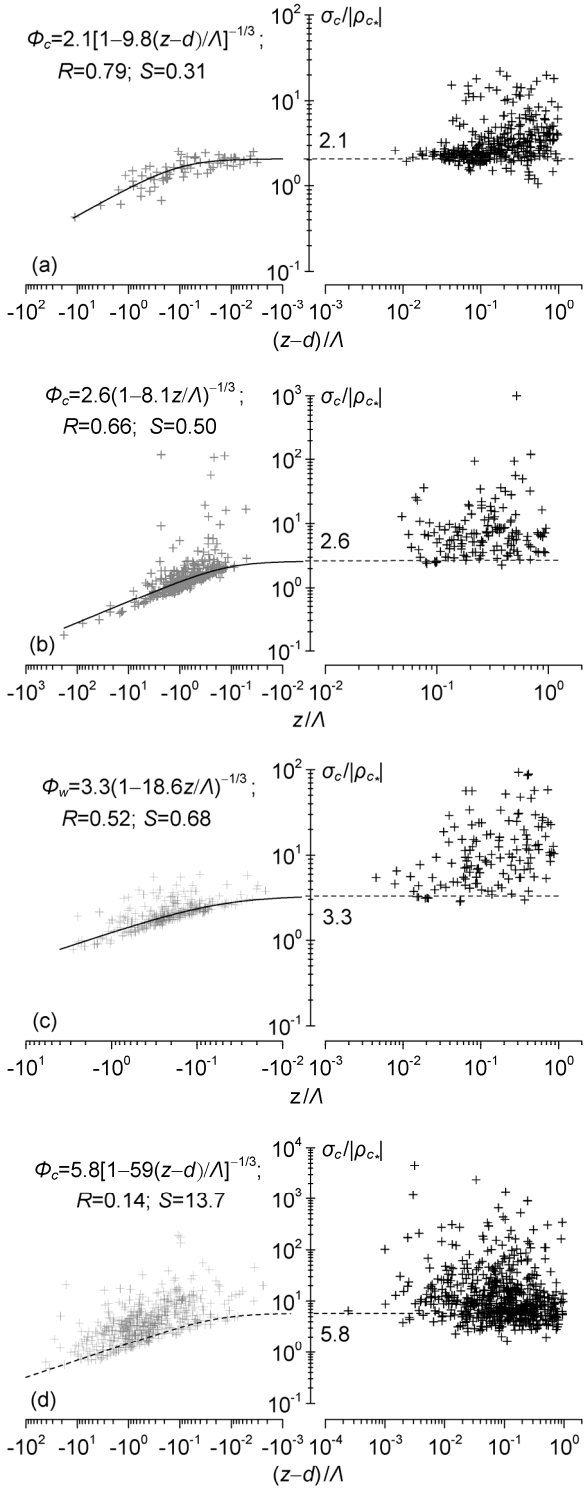

Figure 7 the M-O scaling for CO_2 at level of 10 m (a) in the oasis,10 m (b) and 1.84 m (c) in the Gobi Desert, and 3.08 m (d) in Naqu.

The CO_2 variance in Naqu, in spite of having a homogeneous surface, clearly deviates from the M-O scaling, due to the influence of the cow and sheep in the area. Therefore, the dotted line presents the fitting curve in accordance with the humidity variance (for details see the analysis in Section 3.2.4), along with the relevant correlation coefficient and dispersion variance. Under the condition of stable stratification, the dispersion of CO_2 variance in both the oasis and Gobi Desert is large and irregular, which is in accordance with the results of the temperature variance. However, in

contrast with temperature, the normalized variance of CO_2 deviates from the constant value at the stable stratification predicted when the M-O scaling at the unstable stratification extends to that of the neutral stratification.

3.2.4 M-O scaling properties for humidity

According to the humidity vertical profile of the oasis and Gobi Desert shown in Figure 2, as the source of water vapor, the local circulation carries the water vapor from the oasis to the Gobi Desert, and the humidity in the oasis is 1.0–1.5 times that in the Gobi Desert. Figure 8 shows the analysis results of humidity variance. Under the condition of unstable stratification, the relation of $\sigma_q/|q_*| = 2.1\left[1-8.2(z-d)/\Lambda\right]^{-1/3}$ between the humidity normalization variance of $\sigma_q/|q_*|$ and the stability parameter of $-(z-d)/\Lambda$ can be fitted (Figure 8(a)). This is fully consistent with the M-O scaling for the CO_2 normalization variance in the oasis. The comparison of the humidity with the CO_2 normalization variances at the level of 10 m in the oasis shown in Figure 9 further suggests that, although the vertical turbulence of CO_2 and water vapor in the oasis face opposite directions, their M-O scalings are coincidental. It may be assumed that the Gobi Desert humidity normalization variance of $\sigma_q/|q_*|$ possesses a similar form as that of the oasis, if not affected by the water vapor advection. Figure 8(b) and (c) shows that both humidity normalization variances of $\sigma_q/|q_*|$ at the levels of 10.0 and 1.84 m in the Gobi Desert have an upward dispersion from the M-O scaling. In order to compare the degree of the dispersion, the dotted line draws out the M-O scaling curve for the humidity variance, referring to the CO_2 relations of $\sigma_c/|\rho_{c*}| = 3.3\left(1-18.6\,z/\Lambda\right)^{-1/3}$ and $\sigma_c/|\rho_{c*}| = 2.6(1-8.1\,z/\Lambda)^{-1/3}$ in the Gobi Desert. By comparison, these humidity variances are generally larger than the predicted values of the M-O scaling. Under the condition of stable stratification, both the results of the humidity variance and CO_2 variance are opposite to the results of the temperature variance, and the observation values clearly deviate in the upward direction from the constant value at the stable stratification predicted when the M-O scaling of the unstable stratification extends to that of the neutral stratification.

By synthesizing the deviations of the temperature, humidity, and CO_2 from M-O scaling, it is indicated that, under the condition of unstable stratification, the M-O scaling is valid for the temperature of the oasis although its normalized variance, $-\sigma_\theta/\theta_*$, is great; however, the humidity normalized variances of the Gobi Desert not only are great, but also deviate far from the prediction of the M-O scaling. The M-O scaling is valid for the humidity of the oasis, the temperature of the Gobi Desert, and the CO_2 at the two observational sites. Under the condition of stable stratification, all the scalars deviate from the prediction of the M-O scaling, for both the heterogeneous surface of the oasis-Gobi area and the homogeneous surface of Naqu. In order to eliminate the interference of unknown factors and reasona-

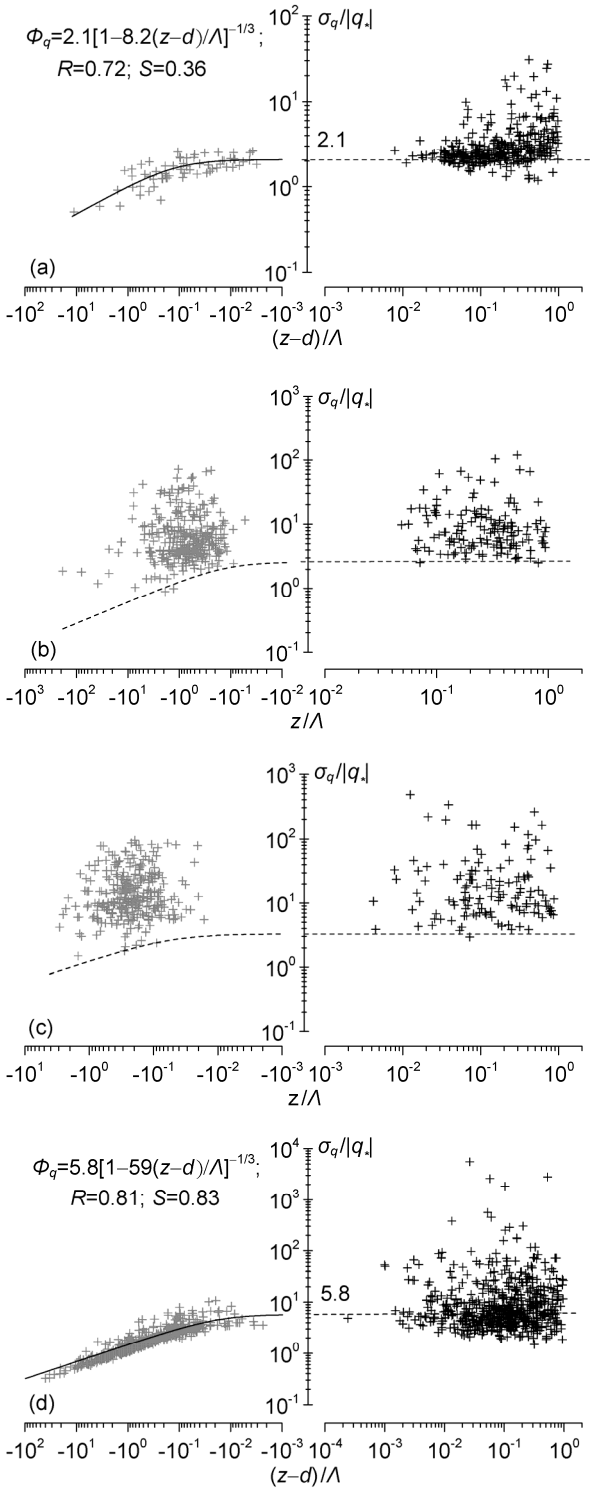

Figure 8 The M-O scaling for humidity at the level of 10 m (a) in the oasis,10 m (b) and 1.84 m (c) in the Gobi Desert, and 3.08 m (d) in Naqu.

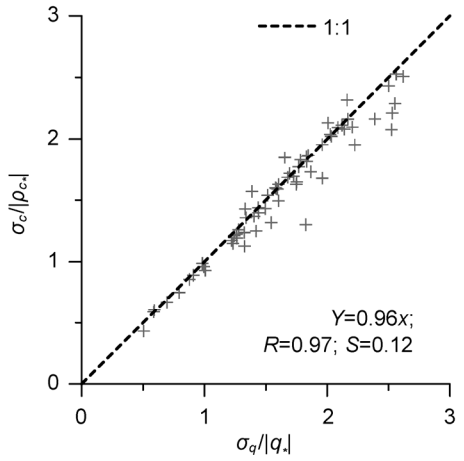

Figure 9 Comparison between humidity and CO_2 normalization variances at 10 m in the oasis.

bly analyze the influence mechanism of advection on the turbulence, the following section will only use the data collected under the condition of unstable stratification.

3.3 Spectrum characteristics of turbulence in the oasis and Gobi Desert

The objective of this section is to reveal the basic characteristics of the oasis and Gobi Desert turbulence spectrum, and analyze the mechanism of the M-O scaling. The following section makes a comparison among the characteristics of the power spectra. The correlation coefficient spectra and Ogive functions of the cospectra are shown to be related to the vertical velocity, temperature, humidity, and CO_2 under the condition of typical unstable stratification with stronger turbulence development at 12:00–13:00 (Beijing time) on June 12 in the oasis and Gobi Desert. In order to perform the comparative analysis with the results of the homogeneous surface, we also list the same spectra and functions under similar conditions at 11:00–12:00 on August 7 in Naqu.

Figure 10 presents the power spectra of the vertical velocity and scalars, such as temperature, humidity, and CO_2 at the level of 10 m in the oasis and Gobi Desert, in which the stability in the oasis is $(z-d)/\Lambda$=–0.01 and that in the Gobi Desert is z/Λ=–0.46. The results suggest that all of the power spectra of the turbulent variables in the inertial range conform to the "–5/3" power law.

Figure 11 presents the Ogive function and correlation coefficient spectra between the vertical velocity and one of scalars, which corresponds to Figure 10. In the figure, (a) and (b) are the Ogive function and correlation coefficient spectrum for the temperature in the oasis and Gobi Desert, respectively; (c) and (d) are the corresponding function and spectrum related to CO_2; and (e) and (f) are the corresponding function and spectrum for humidity. In order to perform a comparison, (a), (b) and (c) in Figure 12 present the Ogive functions and correlation coefficient spectra for temperature, CO_2 and humidity under the condition of stability $(z-d)/\Lambda$=−1.22 in Naqu. A comparison of Figure 11 with Figure 12 shows that the Ogive function and correlation coefficient spectrum have the following characteristics:

(1) Under the condition of unstable stratification, the Ogive function related to temperature and humidity in the oasis and Gobi Desert is an increasing function with the decline of frequency, and the Ogive function for CO_2 shows a decreasing function with the decline of frequency. In theory, the Ogive function tends to converge with the decline of frequency (Figure 12) (Oncley et al., 1996). As shown in Figure 11, all the Ogive functions are related to CO_2 in the oasis and Gobi Desert, the temperature in the Gobi Desert and humidity in the oasis converge and trend to a certain constant value. Moreover, in the low frequency of convergence, the Ogive function for temperature in the oasis is characterized by fluctuation and the Ogive function for humidity in the Gobi Desert presents a sharp oscillation. It is then concluded that both the low frequency turbulent parts related to the above temperature and humidity have significant influences on their fluxes.

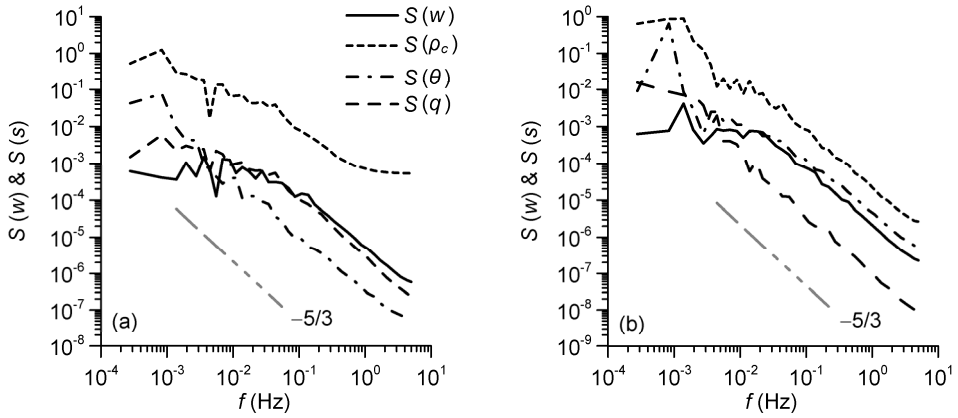

Figure 10 Power spectra of vertical velocity and scalars, such as temperature, humidity, and CO_2 at the level of 10 m in the oasis (a) and Gobi Desert (b).

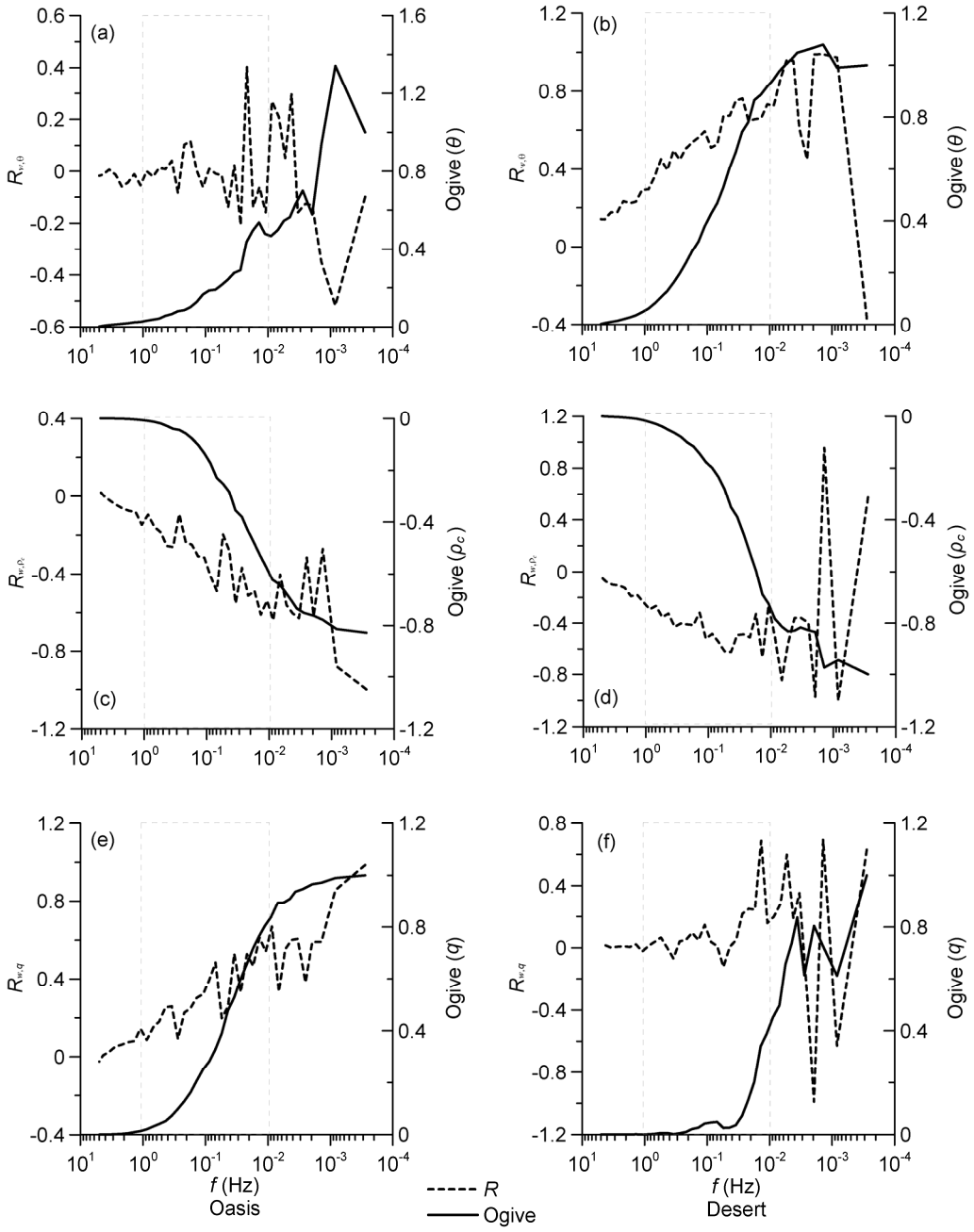

Figure 11 Ogive cumulative frequency spectra and correlation coefficient spectra at the level of 10 m in the oasis and Gobi Desert; (a), (c) and (e) respectively represent the temperature, CO_2 and humidity in the oasis, in which the corresponding stability is $(z-d)/\Lambda$=–0.01; (b), (d) and (f) are those for the same scalars under the condition of stability z/Λ=–0.46 in the Gobi Desert.

(2) Under the condition of homogeneous surface in Naqu, the correlation coefficient spectra for temperature and humidity first increase with the decline of frequency and the increase of Ogive function. When the frequency is less than 10^{-2} Hz, the Ogive function trends to converge, and the correlation coefficient decreases with the decline of frequency (Jiang et al., 2013; McBean et al., 1972). The correlation coefficient for CO_2 is similar to the above variation trend regardless of the minus sign. As far as the heterogeneous surface is concerned, the correlation coefficient spectra for the oasis humidity and Gobi Desert temperature first increases with the decreased frequency and increased Ogive function. When the frequency is less than 10^{-2} Hz, the Ogive function for humidity in the oasis trends to converge, and that for temperature in the Gobi Desert decreases at the lowest frequency. At the same time, the correlation coefficient for humidity in the oasis first decreases slightly, then increases with the decline of frequency, and the correlation coefficient for temperature in the Gobi Desert varies slightly with the decline of frequency. In addition, the values of the

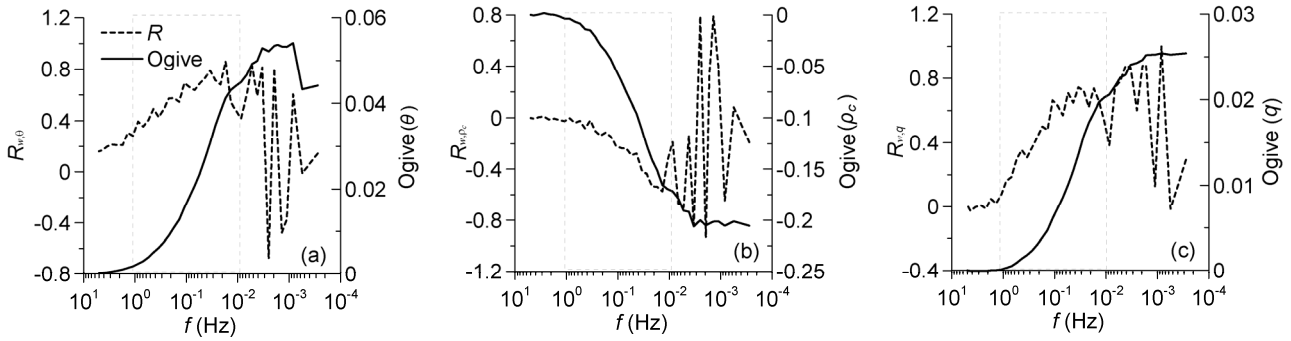

Figure 12 Ogive cumulative frequency spectra and correlation coefficient spectra of temperature (a), CO_2 (b) and humidity (c) at the level of 3.08 m in Naqu, with the corresponding stability $(z-d)/\Lambda=-1.22$.

Ogive function and correlation coefficient spectrum related to CO_2 in the oasis have a similar variation trend with humidity of the oasis, except for the opposite minus. However, the trend of the Ogive function and the correlation coefficient spectrum related to CO_2 are similar to the results observed in Naqu. With regard to the temperature in the oasis and humidity in the Gobi Desert, the relevant correlation coefficient spectra fluctuate between the positive and negative values, with a decline of frequency occurring in the range of 10^1–10^{-2} Hz. The corresponding Ogive function increases with a smaller gradient. In addition, when the frequency is less than 10^{-2} Hz, the gradient of its Ogive function increases rapidly and its correlation coefficient spectrum still fluctuates widely between positive and negative values.

(3) The Ogive function for a scalar following the M-O scaling first increases and then converges with the decline of frequency, which signifies that the high frequency part greater than 10^{-2} Hz has a larger contribution to its Ogive function, and the low frequency part has a smaller contribution. On the contrary, the Ogive function for CO_2 is a decreasing function with the decline of frequency, and the high-frequency part has a larger contribution to the Ogive function, whereas the opposite is true for the low-frequency part. The low-frequency integral part of the Ogive function corresponds to the advection response, advection material transfer, and energy flux. In terms of the definition of the Ogive function, the low frequency part has a great contribution to the Ogive function, which signifies that the low frequency has a significant influence on the covariance between the vertical velocity and turbulent scalar. In other words, the low frequency has a great influence on the vertical turbulent flux. The Ogive function tends to converge to a constant value with the decline of the frequency. A rapid convergence signifies that the influence of the low frequency on the covariance between the vertical velocity and turbulent scalar is disappearing rapidly and converging slowly, which in turn signifies that the same influence is continuous and significant. Therefore, the low frequency has a great contribution to the Ogive function in terms of temperature and humidity, and a small contribution to the Ogive function for CO_2, which signifies that the advection has a great contribution to the sensible and latent heat fluxes and a small contribution to the vertical flux of the CO_2. The Ogive functions related to the temperature of the oasis and the humidity of the Gobi Desert present a fluctuation with the decline of frequency, which shows that the advection has a greater influence on the sensible heat flux in the oasis and latent heat flux in the Gobi Desert.

3.4 Influence of advection from oasis on the humidity variance in the Gobi Desert

Both the vector variance and scalar variance quantify their turbulent intensity. Under the conditions of steady state and homogeneous surface, the MOST reveals the relationship among the turbulent intensities of vertical velocity and scalar intensity and the concerned turbulent flux (Hill, 1989). Over the heterogeneous surface, the causes of the scalar variance deviating from the M-O scaling may provide some clues to reveal the turbulent transporting mechanism. Therefore, the following section will study the possible mechanism of the local advection transporting the turbulent scalar variance by using the observational data of the upstream and downstream in the oasis and Gobi Desert.

First, the data from the sector of wind direction 275°–345° at the Gobi Desert site where the upstream area is located at about the same location as the oasis site are selected (Figure 1). When both the oasis and Gobi Desert are under the condition of unstable stratification, the humidity variance $\sigma_{q\mathrm{B}}$ spurred by the turbulent flow field of the Gobi Desert is estimated by using relation (17) and the observation values of $q_{*\mathrm{B}}$, in which the parameter in $\varphi_{q\mathrm{B}}(z/\Lambda)$ uses the coefficient of CO_2 normalized variance $\sigma_c/|\rho_{c*}| = 3.3[1-18.6\,z/\Lambda]^{-1/3}$ in the Gobi Desert, because the normalized variances of the humidity and CO_2 have the same function relationship under the condition of smaller interference of advection in the oasis. Therefore, the func-

tion relationships of the humidity and CO_2 normalized variances in the Gobi Desert will be the same regardless of the interference of advection. Then, based on the relation (18), the water vapor variance of in the oasis $D\sigma_{q\mathrm{A}}$ after advection transporting and attenuating can be estimated. Figure 13 is a demonstration of the humidity variance, $\sigma_{q\mathrm{A}}$, and the water vapor variance of $D\sigma_{q\mathrm{A}}$ that varies with the stability parameters of $-(z-d)/\Lambda$ after the advection transportation and attenuation. The results indicate that the humidity variance after attenuating basically meets the function relationship of $D\sigma_{q\mathrm{A}}\sim[(z-d)/\Lambda]^{-1/3}$. There is a certain amount of deviation from the function relationship for the different attenuation rates, but the results show an essential improvement compared to Figure 8(b). Figure 14(a) and (b) shows that attenuation rate D varies with the wind velocity and stability parameter of z/Λ, in which the predicted results of relation (21) are valid. The attenuation rate, D, increases with the increasing wind velocity and decreases with the increasing stability parameter of z/Λ. In addition, we also estimated the $D\sigma_{q\mathrm{A}}$ by using the assumption of $\sigma_{sm}^2=\left(\sigma_{s\mathrm{A}}^2+\sigma_{s\mathrm{B}}^2\right)/2$, and the result showed that attenuation rate D was greater than 1, which clearly violates the attenuation law of physics.

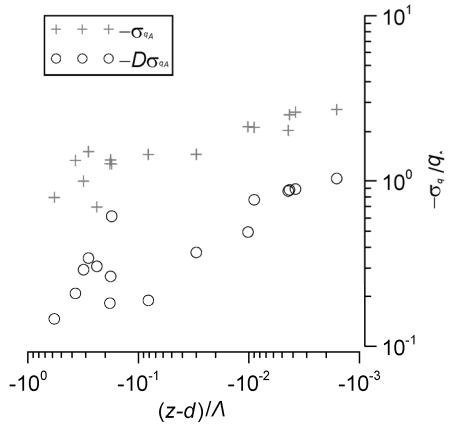

Figure 13 Variation of humidity normalization variance with $(z-d)/\Lambda$ before and after.

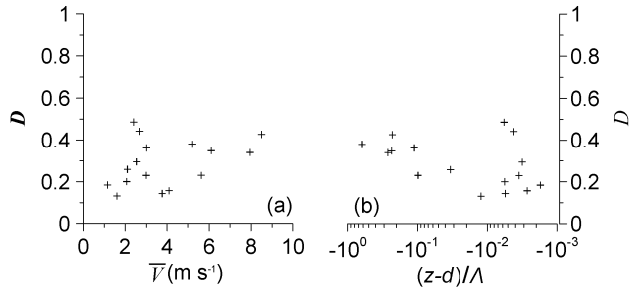

Figure 14 Attenuation rate D of humidity variance originating from the oasis varies with the average velocity (a) and the stability parameters of $(z-d)/\Lambda$ (b).

4 Discussion

In light of the "endogenous factor" and "exogenous factor" scheme proposed by Detto et al. (2010) and the above results, the following inferences may be made. After advection carrying hot air from the Gobi Desert to the oasis, the air in the oasis is affected by a strong turbulent pulse and the temperature variance of the oasis is increased, which may temporarily be referred to as the "exogenous factor" temperature variance of $\sigma_{\theta\mathrm{ex}}=\sqrt{\overline{\theta'^{\,2}_{\mathrm{desert}}}}$. At the same time, the "endogenous factor" temperature variance of $\sigma_{\theta\mathrm{en}}=\sqrt{\overline{\theta'^{\,2}_{\mathrm{oasis}}}}$ is the result of the local flow field and thermal stratification. Affected by the thermal advection and roughness of the surface, the atmosphere in the oasis with more stable stratification and larger friction velocity of u_* has a relatively small turbulent characteristic temperature of θ_*. Because $\sigma_{\theta\mathrm{ex}}$ is much larger than $\sigma_{\theta\mathrm{en}}$ in the components of σ_θ, the $-\sigma_\theta/\theta_*$ of air has a large magnitude. As a factor generating the turbulent flow field, the temperature is affected by advection while its variance still meets the structure of $[-(z-d)/\Lambda]^{-1/3}$. On the contrary, the relatively cold air from the oasis possesses a smaller temperature variance, and the cold advection strengthens the instability of the Gobi Desert atmosphere. The temperature variance of the oasis is relatively small in comparison to that of the Gobi Desert local turbulence, so that the "exogenous factor" temperature variance has little contribution to the temperature variance. The result is that the Gobi Desert air still meets the theory of $(-z/\Lambda)^{-1/3}$, even with a slight deviation. The water vapor of the Gobi Desert originates from the oasis, and thus the "exogenous factor" humidity variance of $\sigma_{q\mathrm{ex}}=\sqrt{\overline{q'^{\,2}_{\mathrm{oasis}}}}$ constitutes the greatest part of the humidity variance. Under the condition of low humidity, however, the "endogenous factor" humidity variance of $\sigma_{q\mathrm{en}}=\sqrt{\overline{q'^{\,2}_{\mathrm{desert}}}}$ is caused by the local turbulent flow field, which has a smaller magnitude. Therefore, the humidity normalization variance of the Gobi Desert is far greater than the prediction of the M-O scaling. Similar to temperature, the opposite dry-air in the Gobi Desert can cause a relatively small deviation of the humidity variance in the oasis, but cannot change its function relationship. Both the CO_2 normalization variances in the oasis and Gobi Desert basically meet the M-O scaling, due to the small difference between the CO_2 variance of the two observation sites. However, the reason why the CO_2 variance at the level of 10 m in the Gobi Desert deviates from the M-O scaling may be the great difference between the CO_2 in the oasis and Gobi Desert, thus there appears to be a similar mixture process of humidity.

5 Conclusions

Under the condition of complex surface in the oasis and Gobi Desert, there exist large differences between the temperature and water vapor of these two areas. In the oasis, the temperature variance at unstable stratification meets the function relationship of $\alpha_\theta[(z-d)/\Lambda]^{-1/3}$, due to the influence of local advection, whereas the magnitude of $-\sigma_\theta/\theta_*$ increases compared to its magnitude, under the condition of homogeneous surface. Under the same conditions, the humidity variance and CO_2 variance both meet the conditions of relation (5). In the Gobi Desert, the temperature variance meets relation (7) and the CO_2 variance meets relation (5), while the humidity variance significantly deviates from the M-O scaling. There exists little difference in terms of CO_2 between the oasis and Gobi Desert, and thus the advection has little influence on the M-O scaling for CO_2. Almost all water vapor in the Gobi Desert originates from the advection transport of the oasis, and as a result the characteristics of the oasis humidity variance are partly preserved and have a significant influence on the Gobi Desert humidity variance. After discussion, the M-O scaling of the scalar turbulence is determined by the magnitude of scalar variance transported by advection, which is the relative size of "exogenous factor" variance and "endogenous factor" variance. If the "exogenous factor" scalar variance transported by the advection is quite large, then the observation value of the scalar variance will deviate from the M-O scaling. When the "endogenous factor" scalar variance is very large, then the M-O scaling for the scalar is valid.

This study was supported by the National Basic Research Program of China (Grant No.2010CB951701-2), the National Natural Science Foundation of China (Grant Nos. 91025011, 41130961), and the Pingliang Station of Lightning and Hail Research, Cold and Arid Regions Environmental and Engineering Research Institute, Chinese Academy of Sciences. We especially thank Miao Desui for help.

Ao Y, Lü S, Chen S, et al. 2005. Analyses of cold wet tongue and boundary layer characteristics inside and outside of Jinta oasis (in Chinese). Plateau Meteorol, 24: 503–508

Asanuma J, Brutsaert W. 1999. The effect of chessboard variability of the surface fluxes on the aggregated turbulence fields in a convective atmospheric surface layer. Bound-Layer Meteorol, 91: 37–50

Chen J, Lü S, Yu Y. 2012. Comparison of heat and matter transfer characteristics in the surface layers of oasis and Gobi (in Chinese). Chin J Geophys, 6: 1817–1830

De Bruin H A R, Van Den Hurk B J J M, Kroon L J M. 1999. On the temperature-humidity correlation and similarity. Bound-Layer Meteorol, 93: 453–468

Detto M, Katul G, Mancini M, et al. 2008. Surface heterogeneity and its signature in higher-order scalar similarity relationships. Agric For Meteorol, 148: 902–916

Detto M, Baldocchi D, Katul G G. 2010. Scaling properties of biologically active scalar concentration fluctuations in the atmospheric surface layer over a managed peatland. Bound-Layer Meteorol, 136: 407–430

Finnigan J J. 2008. An introduction to flux measurements in difficult conditions. Ecol Appl, 18: 1340–1350

Guo X, Zhang H, Cai X, et al. 2009. Flux-variance method for latent heat and carbon dioxide fluxes in unstable condition. Bound-Layer Meteorol, 131: 363–384

Hill R J. 1989. Implications of Monin-Obukhov similarity theory for scalar quantities. J Atmos Sci, 46: 2236–2244

Högström U, Smedman-Högström A S. 1974. Turbulence mechanisms at an agricultural site. Bound-Layer Meteorol, 7: 373–389

Hu Y, Chen J, Zuo H. 2007. Theorem of turbulent intensity and macroscopic mechanism of the turbulence development. Sci China Ser D-Earth Sci, 50: 789–800

Hu Y Q, Su C X, Zhang Y F. 1988. Research on the microclimate characteristics and cold island effect over a reservoir in the Hexi. Adv Atmos Sci, 5: 117–126

Hu Y, Zhang Q. 1993a. On local similarity of the atmospheric boundary layer (in Chinese). Chin J Atmos Sci, 17: 10–20

Hu Y, Wang J, Zuo H. 1993b. Character of water vapour transportation in the surface layer over desert near oasis (in Chinese). Plateau Meteorol, 12: 125–132

Jiang H, Liu S, Liu H. 2013. A Study on characteristics of cospectra in a disturbed surface layer (in Chinese). Acta Sci Nat Univ Pekinensis, 49: 435–442

Kader B A, Yaglom A M. 1990. Mean fields and fluctuation moments in unstably stratified turbulent boundary layers. J Fluid Mech, 212: 637–662

Kaimal J C, Gaynor J E. 1991. Another look at sonic thermometry. Bound-Layer Meteorol, 56: 401–410

Katul G, Goltz S M, Hsieh C I, et al. 1995. Estimation of surface heat and momentum fluxes using the flux-variance method above uniform and nonuniform terrain. Bound-Layer Meteor, 74: 237–260

Katul G G, Hsieh C I. 1999. A note on the flux-variance similarity relationships for heat and water vapour in the unstable atmospheric surface layer. Bound-Layer Meteorol, 90: 327–338

Lamaud E, Irvine M. 2006. Temperature and humidity dissimilarity and heat-to-water-vapour transport efficiency above and within a pine forest canopy: The role of the Bowen ratio. Bound-Layer Meteorol, 120: 87–109

Mahrt L. 1989. Intermittency of atmospheric-turbulence. J Atmos Sci, 46: 79–95

Mahrt L, Sun J, Blumen W, et al. 1998. Nocturnal boundary-layer regimes. Bound-Layer Meteorol, 88: 255–278

Martano P. 2002. Estimation of surface roughness length and displacement height from single-level sonic anemometer data. J Appl Meteorol, 39: 708–715

McBean G A, Miyake M. 1972. The turbulent transfer mechanisms in the atmospheric surface layer. Quart J R Met Soc, 98: 383–398

McNaughton K G, Laubach J. 1998. Unsteadiness as a cause of non-equality of eddy diffusivities for heat and vapour at the base of an advective inversion. Bound-Layer Meteorol, 88: 479–504

Moene A F, Michels B I, Holtslag A A M. 2006. Scaling variances of scalars in a convective boundary layer under different entrainment regimes. Bound-Layer Meteorol, 120: 257–274

Monin A S, Obukhov A M. 1954. Basic laws of turbulent mixing in the ground layer of the atmosphere. Trans Geophys Inst Akad Nauk USSR, 151: 163–187

Oncley S P, Friehe C A, Larue J C, et al. 1996. Surface-layer fluxes, profiles, and turbulence measurements over uniform terrain under near-neutral conditions. J Atmos Sci, 5: 1029–1044

Padro J. 1993. An investigation of flux-variance methods and universal functions applied to three land-use types in unstable conditions. Bound-Layer Meteorol, 66: 413–425

Panofsky H A, Lenschow D H, Wyngaard J C. 1977. The characteristics of turbulent velocity components in the surface layer under unstable conditions. Bound-Layer Meteorol, 11: 355–361

Ricardo K S, David R F, Kathleen E M. 2001. Importance of low-frequency contributions to eddy fluxes observed over rough surfaces, J Appl Meteorol, 40: 2178–2192

Schotanus P, Nieuwstadt F T M, de Bruin H A R. 1983. Temperature

measurement with a sonic anemometer and its application to heat and moisture fluxes. Bound-Layer Meteorol, 26: 81–93
Shao Y, Hacher J M. 1990. Local similarity relationships in a horizontal inhomogeneous boundary layer. Bound-Layer Meteorol, 52: 17–40
Sorbian Z. 1989. Structure of the Atmospheric Boundary Layer. London: Prentice Hall. 317
Su C, Hu Y, Zhang Y, et al. 1987. The microclimate character and "cold island effect" over the oasis in Hexi region (in Chinese). Chin J Atmos Sci, 11: 390–396
Stull R B. 1988. An Introduction to Boundary-Layer Meteorology. 2nd ed. Dordrecht: Kluwer Academic Publishers. 666
Townsend A A. 1961. Equilibrium layers and wall turbulence. J Fluid Mech, 11: 97–120
Webb E K, Pearman G I, Leuning R. 1980. Correction of the flux measurements for density effects due to heat and water vapour transfer. Q J R Meteorol Soc, 106: 85–100
Wei Z, Lü S, Hu Z, et al. 2005. A primary research on the characteristics of wind, temperature and humidity in the boundary layer over Jinta summer (in Chinese). Plateau Meteorol, 24: 846–856
Wen L, Lü S, Zhang Y, et al. 2005. Numerical simulation and structure analyses of the local circulation in jinta oasis summer (in Chinese). Plateau Meteorol, 24: 478–486
Wyngaard J C, Coté O R, Izumi Y. 1971. Local free convection, similarity and the budgets of shear stress and heat flux. J Atmos Sci, 28: 1171–1182
Zhang Q, Hu Y, Wang X. 1992. The characters of micrometeorology on farmland in oasis in Heihe region (in Chinese). Plateau Meteorol, 11: 361–370
Zhang Q, Hu Y. 2001. Scientific problems and advance of atmospheric boundary layer physics. Adv Earth Sci, 16: 526–532